Published in final edited form as:
Science. 2012 March 16; 335(6074): 1359–1362. doi:10.1126/science.1215909.

ER Cargo Properties Specify A Requirement For COPII Coat Rigidity Mediated By Sec13p[§]

Alenka Čopič[†], **Catherine F. Latham**[†], **Max A. Horlbeck**, **Jennifer G. D'Arcangelo**, and **Elizabeth A. Miller**[*]
Department of Biological Sciences, Columbia University, New York, NY 10027. USA

Abstract

Eukaryotic secretory proteins exit the endoplasmic reticulum via transport vesicles generated by the essential COPII coat proteins. The outer coat complex, Sec13-Sec31, forms a scaffold that is thought to enforce curvature. By exploiting yeast bypass-of-sec-thirteen (*bst*) mutants, where Sec13p is dispensable, we probed the relationship between a compromised COPII coat and the cellular context in which it could still function. Genetic and biochemical analyses suggested that Sec13p was required to generate vesicles from membranes that contained asymmetrically distributed cargoes that were likely to confer opposing curvature. Thus Sec13p may rigidify the COPII cage and increase its membrane-bending capacity; this function could be bypassed when a *bst* mutation renders the membrane more deformable.

Hierarchical assembly of the COPII coat on the cytosolic face of the endoplasmic reticulum (ER) membrane couples cargo selection with membrane deformation to generate functional transport vesicles (1). All members of the COPII coat are thought to contribute to generation of membrane curvature (2, 3); however the precise mechanism of membrane deformation by the COPII coat remains unclear (4). We sought to probe this process by dissecting the molecular function of the outer coat complex, composed of Sec13 and Sec31, which is thought to drive membrane curvature by polymerization into a lattice-like spherical structure (3). Sec13 is unique among COPII proteins in performing multiple functions, driven by structurally analogous interactions with distinct partners, including its canonical partner, Sec31 (5), the nucleoporin, Nup145 (6), and the COPII scaffold, Sec16 (7). Given the pleiotropic functions of Sec13 and the essential nature of COPII-mediated traffic, it is surprising that yeast Sec13p is dispensable in the context of bypass-of-sec-thirteen (*bst*) mutations (8, 9). We sought to exploit this phenotype to probe vesicle formation in the context of a compromised coat complex.

The COPII "cage" self-assembles from rod-shaped Sec13-Sec31 "edge" elements, four of which come together at "vertex" regions (3). Sec31 is thought to drive assembly: the edge element is formed by stable dimerization at the α-solenoid "ancestral coat element" (ACE)

[*]To whom correspondence should be addressed. em2282@columbia.edu.
[†]These authors contributed equally to this work.

Supporting Online Material.
Materials and Methods
Figs. S1 – S8
Table S1 and S2
References 32 – 42

Additional data described in the manuscript are presented in the Supporting Online Material.

domain; four edge elements come together at cage vertices via N-terminal β-propellers (5). Sec13 lies sandwiched between the ACE and β-propeller domains, forming a 6-bladed β-propeller that is complemented by an additional β-blade formed by the "domain insertion motif" (DIM) of Sec31 (Fig. 1A). We first demonstrated that the essential function of yeast Sec13p was in the COPII coat by restricting its interaction to Sec31p (10): an in-frame fusion where Sec13p was inserted immediately downstream of the Sec31p DIM complemented both *sec13Δ* and *sec31Δ* strains, whereas a fusion containing the Sec13p structural homolog, Seh1p, was unable to support viability (Fig. 1B) despite being functional in a *bstΔ* background (Fig. S1). Furthermore, uncoupling Sec13p from the COPII coat via mutation of the Sec31p DIM, either by point mutations (*sec31-DK*) or by complete replacement with a 13 amino acid stretch of Gly-Ser repeats (*sec31-GS$_{13}$*), failed to support viability except in the context of an additional *bst1Δ* mutation (Fig. 1C), effectively mimicking a *sec13Δ* mutation. We tested whether Sec31p could engage with the COPII coat independent of Sec13p. Indeed, Sec31p, expressed and purified from insect cells to preclude co-purification of Sec13p, was efficiently recruited to synthetic liposomes in the presence of the inner COPII coat, Sar1p-Sec23p-Sec24p (Fig. 1D). Furthermore, the Sec31p DIM mutants also assembled with the inner coat but were unable to recruit Sec13p (Fig. 1D). Finally, we used an in vitro vesicle formation assay (11) to confirm that Sec31p was sufficient to generate COPII vesicles in the absence of Sec13p, albeit with reduced efficiency (Fig. 1E).

If Sec31p can generate COPII vesicles on its own, what is the molecular function of Sec13p and what are the in vivo conditions created by the *bst* mutations that permit Sec31p function in its absence? We used synthetic genetic array technology (12) to exhaustively survey the yeast genome for *BST* genes. Two query mutations - *sec31-GS$_{13}$* and *sec13Δ* - were introduced into the yeast deletion collection and haploid double mutants scored for viability (Fig. 2A and Fig. S2). Three comprehensive screens yielded 118 preliminary hits, 30 of which were identified using both query strains (Fig. 2A, Table S1). Many of these overlapping hits were false positives and a few were ambiguous because their phenotypes were too weak to be conclusively confirmed (Fig. 2A and Fig. S3). Our screens thus yielded 7 "core" *bst* mutants and by direct testing we identified 3 additional functionally related hits (Fig. 2A–C).

The majority of *BST* gene products fell into two functional categories (Fig. 2B): Bst1p, Ted1p, Per1p and Gup1p are ER enzymes that catalyze remodeling of glycosylphosphatidylinositol (GPI) anchors after proteins have been covalently attached (13, 14); Emp24p, Erv25p, Erp1p and Erp2p are members of the p24 family and form a physical complex that shuttles between the ER and Golgi and is required for efficient ER export of GPI-anchored proteins (GPI-APs) (9, 15, 16). Maturation of the GPI-AP, Gas1p, was defective in each of these two classes of *bst* mutants (Fig. 2D and ref. (17); in the case of the p24 mutants, the strength of the GPI-AP defect mirrored the strength of the *bst* phenotype (Fig. 2C–D and Fig. S4A–B). Two final "core" *BSTs* were *YGL024w*, a dubious ORF (Fig. S5), and *ERV29*, an ER export receptor for soluble cargo proteins (18, 19). *ERV29* deletion conferred a weak *bst* phenotype that was potentiated by additional disruption of *ERP1* (Fig. 2C). Although Erv29p does not participate directly in the trafficking of GPI-APs (18), an *erv29Δ* mutation exacerbated the Gas1p processing defect observed in *erp1Δ* cells (Fig. 2D and Fig. S4A).

Since most core *bst* mutants shared defects in ER export of Gas1p, we considered the possibility that broad depletion of non-essential cargoes could permit more efficient capture of essential proteins, enabling cell survival even when the COPII coat is compromised. However, maturation of the soluble vacuolar hydrolase, CPY, was normal in *bst* mutant strains (Fig. 2D and Fig. S4C), suggesting that the *bst* mutations do not generally enhance

secretion. Furthermore, all of the known cargo adaptors were screened in our genetic analyses, yet only the p24 proteins and Erv29p arose as hits (Table S1), suggesting that there is something unique about the cargo molecules handled by these proteins that permits deletion of Sec13p. Both GPI-APs and p24 proteins are particularly abundant (20) and highly asymmetrical membrane proteins, with the bulk of their mass residing exclusively (GPI-APs) or predominantly (p24s) in the ER lumen. Localized concentration of such asymmetrically distributed cargoes could alter the physical properties of the membrane by steric or entropic mechanisms and oppose the curvature enforced by the COPII coat by virtue of this topology (Fig. S6). This model could also explain the *bst* phenotype of *erv29Δ*, since Erv29p becomes asymmetric when bound to its soluble clients. The decrease in local concentration of cargoes associated with *bst* mutants could lower the membrane bending energy such that the COPII coat could act in the absence of Sec13p (Fig. S7). Two major curvature-inducing ER membrane proteins, Rtn1p and Yop1p (21), did not impact viability of a *bst1Δ sec13Δ* strain (Fig. 3A), suggesting global curvature of the ER membrane is unrelated to Sec13p bypass. Furthermore, deletion of the very long chain fatty acid elongases, Sur4p or Fen1p, reversed the viability of the *bst1Δ sec13Δ* strain but not the *bst1Δ sec31-DK* strain (Fig. 3B), suggesting that these lipid species modulate curvature at the nuclear pore, where Sec13p functions in complex with Nup145 (6), rather than in COPII vesicles (22). Thus *BST* genes appear to specifically influence membrane properties at the sites of vesicle formation.

Our genetic data point to a role for Sec13p in generating vesicles from membranes that contain the full complement of asymmetrically distributed proteins, cargoes that may confer significant local negative spontaneous curvature. We tested whether Sec13p contributes rigidity to the Sec31p rods such that cage polymerization can exert sufficient force on the ER membrane to overcome the membrane bending energy of this asymmetric membrane. We deleted the flexible region that links the ACE and β-propeller domains of Sec31p, creating an edge element that might be expected to exhibit structural rigidity conferred by direct apposition of the two domains (Fig. 4A). Indeed, the corresponding mutant, *sec31-Δhinge*, supported viability independent of a *bst* mutation (Fig. 4B). In contrast, deletion of the DIM alone, which preserves a short flexible domain and a disordered loop missing from the crystal structure, did not suffice for viability (7) unless an additional *bst* mutation was present (*sec31-Δblade* in Fig. 4B). The purified Sec31p-Δhinge protein assembled on synthetic liposomes (Fig. 4C), suggesting robust functionality. In cells expressing only this rigidified form of Sec31p, Sec13p-GFP redistributed from large ER exit sites to a diffuse cytosolic localization with a coincident increase in nuclear envelope fluorescence (Fig. 4D). Small residual puncta may have reflected a Sec16p-associated pool of Sec13p (7), which is not required for viability since, remarkably, *SEC13* could be deleted entirely when Sec31p-Δhinge was expressed (Fig. 4E). ER exit sites, as marked by Sec24p-GFP, were normal in *sec31-Δhinge* mutant cells that lacked Sec13p (Fig. 4D) and secretory protein maturation in vivo was indistinguishable from wild-type cells (Fig. 4F) suggesting that ER export was fully operational in the absence of Sec13p. We tested the effect of converse mutations in Sec31p – those that might decrease rigidity of the Sec13/31p complex by destabilizing the β-propeller interface – and demonstrated that one such mutant was viable only in a *sec31Δ emp24Δ* background despite being able to assemble into a Sec13/31p complex (Fig. S8). We thus propose that Sec13p rigidifies the COPII cage, increasing its membrane bending capacity; when a *bst* mutation creates a donor membrane more permissive to deformation this function of Sec13p is no longer required (Fig. S7).

By exploiting the *bst* phenotype to understand how secretion occurs when the COPII coat is compromised, we determined that cargo sorting can impact vesicle formation. We propose that *bst* mutations create a locally altered membrane that lacks the full complement of asymmetrically distributed cargo proteins such that the membrane can be deformed into a

small vesicle absent the rigidifying effect of Sec13p. Indeed, a truncated form of Sec31p that lacks a flexible domain encompassing the Sec13p interaction motif supports viability in the absence of a *bst* mutation, suggesting that an artificially rigidified coat can exert sufficient force to bend an asymmetric cargo-rich membrane. Membrane bending properties of coat proteins have largely been characterized on synthetic liposomes (23–25), which fail to recapitulate important properties of cellular membranes, including the abundance and complexity of protein cargoes and the asymmetry that lipids and proteins can exhibit across the bilayer. Coat proteins have evolved to overcome the barrier to curvature that such constituents present, employing multiple mechanisms to enforce shape changes (4). The structural rigidity conferred to the COPII coat by Sec13 has parallels in other vesicle transport systems, notably the clathrin coat, where structural models predict that depletion of clathrin light chain renders the heavy chain triskelion more flexible yet still competent for vesicle formation (26). The presence of Sec13 within the COPII cage may also permit multiple geometries, allowing the coat to adapt to cell- or condition-specific cargo packaging requirements (27). Indeed, mammalian cells depleted of Sec13 show collagen-specific trafficking defects (28) that may reflect the inability of a Sec13-free coat to adequately deform the membrane around a uniquely rigid cargo. Furthermore, ER export of large cargoes requires alternative COPII subunits like the yeast Sec24p paralog, Lst1p/Sfb2p, which facilitates traffic of the abundant oligomeric Pma1p complex (29, 30), or accessory factors such as human TANGO1, which promotes trafficking of pro-collagen (31). Such accessory proteins could influence membrane properties to either oppose the force of the COPII coat, preventing premature vesicle scission, or augment curvature conferred by the coat to ensure encapsulation of a rigid cargo. In addition to large and rigid cargoes, we propose that proteins with particularly asymmetric topologies will also influence the mechanics of vesicle formation.

Supplementary Material

Refer to Web version on PubMed Central for supplementary material.

Acknowledgments

We thank J. Goldberg, C. Boone, E. Snapp and M. Lee for strains and reagents; T. Swayne, E. Bauer, R. Rothstein, J. Dittmar and members of the Rothstein lab for technical assistance; and B. Antonny, J. Derganc, M. Lee and F. Pincet for valuable discussions. This work was supported by a Columbia RISE award and NIH grants GM085089 and GM078186 to EAM and by a Columbia Frontiers of Science fellowship to AC. MH was an I.I. Rabi Science Scholar of Columbia University.

References and Notes

1. Miller EA, Barlowe C. Regulation of coat assembly--sorting things out at the ER. Curr Opin Cell Biol. 2010; 22:447. [PubMed: 20439155]
2. Bi X, Corpina RA, Goldberg J. Structure of the Sec23/24-Sar1 pre-budding complex of the COPII vesicle coat. Nature. 2002; 419:271. [PubMed: 12239560]
3. Stagg SM, et al. Structure of the Sec13/31 COPII coat cage. Nature. 2006; 439:234. [PubMed: 16407955]
4. Zimmerberg J, Kozlov M. How proteins produce cellular membrane curvature. Nat Rev Mol Cell Biol. 2006; 7:9. [PubMed: 16365634]
5. Fath S, Mancias JD, Bi X, Goldberg J. Structure and organization of coat proteins in the COPII cage. Cell. 2007; 129:1325. [PubMed: 17604721]
6. Brohawn SG, Schwartz TU. Molecular architecture of the Nup84-Nup145C-Sec13 edge element in the nuclear pore complex lattice. Nat Struct Mol Biol. 2009; 16:1173. [PubMed: 19855394]
7. Whittle JRR, Schwartz TU. Structure of the Sec13-Sec16 edge element, a template for assembly of the COPII vesicle coat. J Cell Biol. 2010; 190:347. [PubMed: 20696705]

8. Elrod-Erickson MJ, Kaiser CA. Genes that control the fidelity of endoplasmic reticulum to Golgi transport identified as suppressors of vesicle budding mutations. Mol Biol Cell. 1996; 7:1043. [PubMed: 8862519]
9. Marzioch M, et al. Erp1p and Erp2p, partners for Emp24p and Erv25p in a yeast p24 complex. Mol Biol Cell. 1999; 10:1923. [PubMed: 10359606]
10. Full methods are available in the Supporting Online Material.
11. Barlowe C, et al. COPII: a membrane coat formed by Sec proteins that drive vesicle budding from the endoplasmic reticulum. Cell. 1994; 77:895. [PubMed: 8004676]
12. Tong AH, et al. Systematic genetic analysis with ordered arrays of yeast deletion mutants. Science. 2001; 294:2364. [PubMed: 11743205]
13. Fujita M, Jigami Y. Lipid remodeling of GPI-anchored proteins and its function. Biochim Biophys Acta. 2008; 1780:410. [PubMed: 17913366]
14. Fujita M, et al. GPI glycan remodeling by PGAP5 regulates transport of GPI-anchored proteins from the ER to the Golgi. Cell. 2009; 139:352. [PubMed: 19837036]
15. Muniz M, Nuoffer C, Hauri H, Riezman H. The Emp24 complex recruits a specific cargo molecule into endoplasmic reticulum-derived vesicles. J Cell Biol. 2000; 148:925. [PubMed: 10704443]
16. Fujita M, et al. Sorting of GPI-anchored proteins into ER exit sites by p24 proteins is dependent on remodeled GPI. J Cell Biol. 2011; 194:61. [PubMed: 21727194]
17. Copic A, et al. Genomewide analysis reveals novel pathways affecting endoplasmic reticulum homeostasis, protein modification and quality control. Genetics. 2009; 182:757. [PubMed: 19433630]
18. Belden WJ, Barlowe C. Role of Erv29p in collecting soluble secretory proteins into ER-derived transport vesicles. Science. 2001; 294:1528. [PubMed: 11711675]
19. Dancourt J, Barlowe C. Protein sorting receptors in the early secretory pathway. Annu Rev Biochem. 2010; 79:777. [PubMed: 20533886]
20. Ghaemmaghami S, et al. Global analysis of protein expression in yeast. Nature. 2003; 425:737. [PubMed: 14562106]
21. Voeltz GK, Prinz WA, Shibata Y, Rist JM, Rapoport TA. A class of membrane proteins shaping the tubular endoplasmic reticulum. Cell. 2006; 124:573. [PubMed: 16469703]
22. Schneiter R, et al. Identification and biophysical characterization of a very-long-chain-fatty-acid-substituted phosphatidylinositol in yeast subcellular membranes. Biochem J. 2004; 381:941. [PubMed: 15270698]
23. Lee MCS, et al. Sar1p N-terminal helix initiates membrane curvature and completes the fission of a COPII vesicle. Cell. 2005; 122:605. [PubMed: 16122427]
24. Bielli A, et al. Regulation of Sar1 NH2 terminus by GTP binding and hydrolysis promotes membrane deformation to control COPII vesicle fission. J Cell Biol. 2005; 171:919. [PubMed: 16344311]
25. Peter BJ, et al. BAR domains as sensors of membrane curvature: the amphiphysin BAR structure. Science. 2004; 303:495. [PubMed: 14645856]
26. Wilbur JD, et al. Conformation switching of clathrin light chain regulates clathrin lattice assembly. Dev Cell. 2010; 18:841. [PubMed: 20493816]
27. Stagg SM, et al. Structural basis for cargo regulation of COPII coat assembly. Cell. 2008; 134:474. [PubMed: 18692470]
28. Townley AK, et al. Efficient coupling of Sec23-Sec24 to Sec13-Sec31 drives COPII-dependent collagen secretion and is essential for normal craniofacial development. J Cell Sci. 2008; 121:3025. [PubMed: 18713835]
29. Roberg KJ, Crotwell M, Espenshade P, Gimeno R, Kaiser CA. LST1 is a SEC24 homologue used for selective export of the plasma membrane ATPase from the endoplasmic reticulum. J Cell Biol. 1999; 145:659. [PubMed: 10330397]
30. Shimoni Y, et al. Lst1p and Sec24p cooperate in sorting of the plasma membrane ATPase into COPII vesicles in Saccharomyces cerevisiae. J Cell Biol. 2000; 151:973. [PubMed: 11086000]
31. Saito K, et al. TANGO1 facilitates cargo loading at endoplasmic reticulum exit sites. Cell. 2009; 136:891. [PubMed: 19269366]

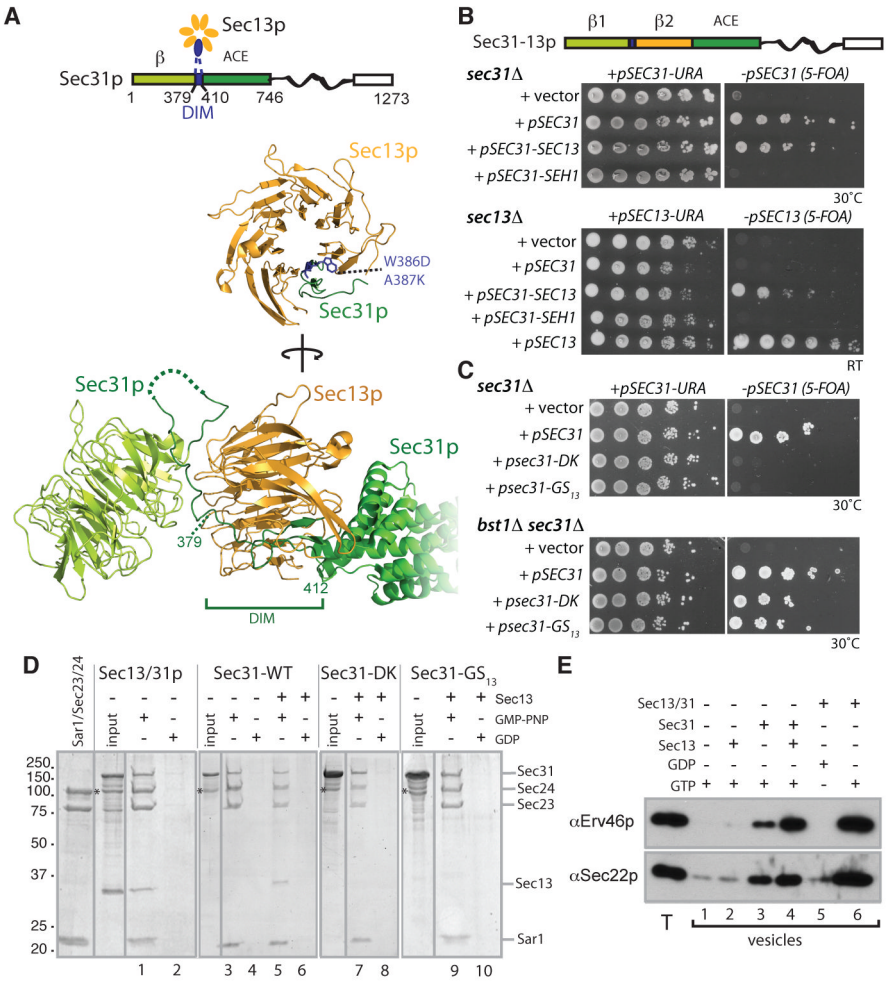

Figure 1. Sec31p mutants mimic the loss of Sec13p

(A) Schematic and structural representations of Sec31p (green) and Sec13p (orange) showing the Sec31p DIM (blue), β-propeller (light green) and ACE (dark green) domains. Residues (W386D and A387K) altered in the Sec31p-DK mutant are indicated and numbering denotes Sec31p residues. **(B)** Schematic of the Sec31-Sec13p fusion, which was introduced into *sec31Δ* and *sec13Δ* strains as indicated and grown on media containing 5-FOA to counterselect for the wild-type plasmid-borne copies of *SEC13* or *SEC31*. **(C)** A *sec31Δ* strain containing a plasmid-borne *sec31-GS*$_{13}$ and *sec31-DK* mutant as the sole copy of *SEC31* was viable only in *bst* mutant backgrounds. **(D)** Synthetic liposomes were incubated with the COPII coat proteins and guanine nucleotides indicated and coat assembly assessed by liposome flotation and SDS-PAGE. Numbered lanes contain liposome-bound proteins; * denotes a degradation product of Sec31p**. (E)** Microsomal membranes (T – 10% of total input membranes) purified from *bst1*Δ cells were incubated with Sar1p and Sec23/24p, supplemented with Sec13p, Sec31p and guanine nucleotides as indicated; vesicles released were purified and analyzed by immunoblotting against cargo proteins Sec22p and Erv46p.

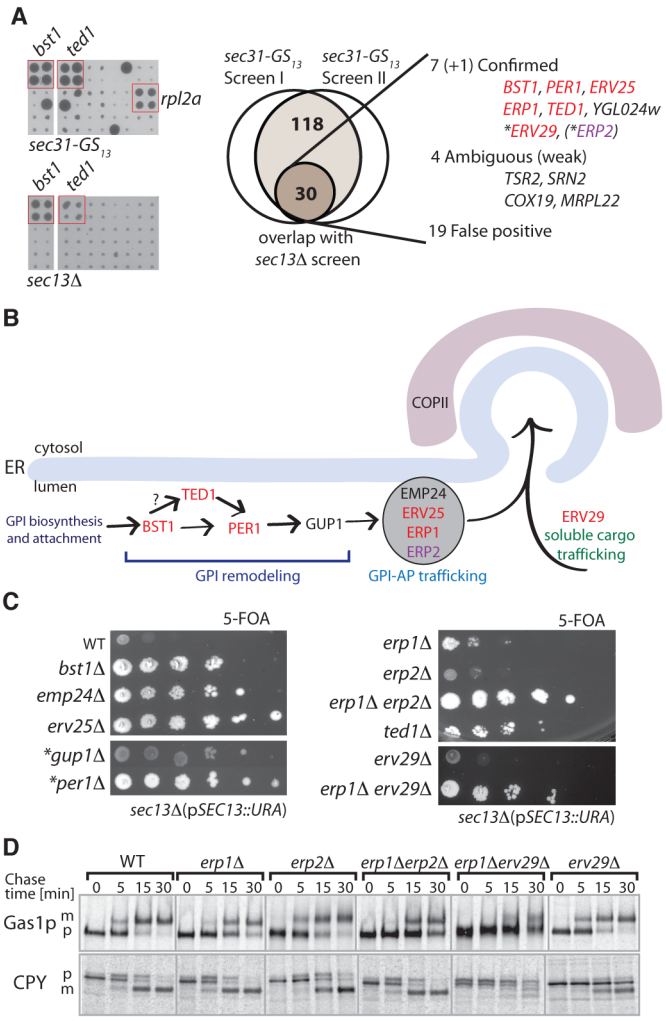

Fig. 2. Strong *bst* mutants affect export of GPI-anchored proteins from the ER

(A) SGA screen summary showing examples of hits (quadruplicate spots are highlighted) on 5-FOA plates (left panel), screen outcomes from two independent *sec31-GS*$_{13}$ screens and overlap with *sec13Δ* screen hits (middle panel), and a list of overlap hits (right panel) that were further confirmed by direct crosses with *sec13Δ* or *sec13Δ erp1Δ* (*) strains. *ERP2* is functionally related to other hits (highlighted in red) but was identified only in *sec31-GS*$_{13}$ screens. **(B)** Most confirmed *BST* genes act in GPI-AP remodeling and trafficking pathways. *EMP24* and *GUP1*, though not identified in the screens, conferred *bst* phenotypes upon direct testing. **(C)** Growth phenotypes of *bstΔ sec13Δ* strains generated by direct crosses on 5-FOA at 25°C. (*) The phenotypes of *gup1Δ sec13Δ* and *per1Δ sec13Δ* depend on the strain background. **(D)** Maturation (trafficking) of the GPI-AP Gas1p in p24 and *erv29Δ* mutants, as revealed by pulse-chase experiments. Maturation of a soluble protein, CPY, is shown for comparison; ‘p’ marks precursor (ER) forms, “m” indicates mature (post-Golgi) forms.

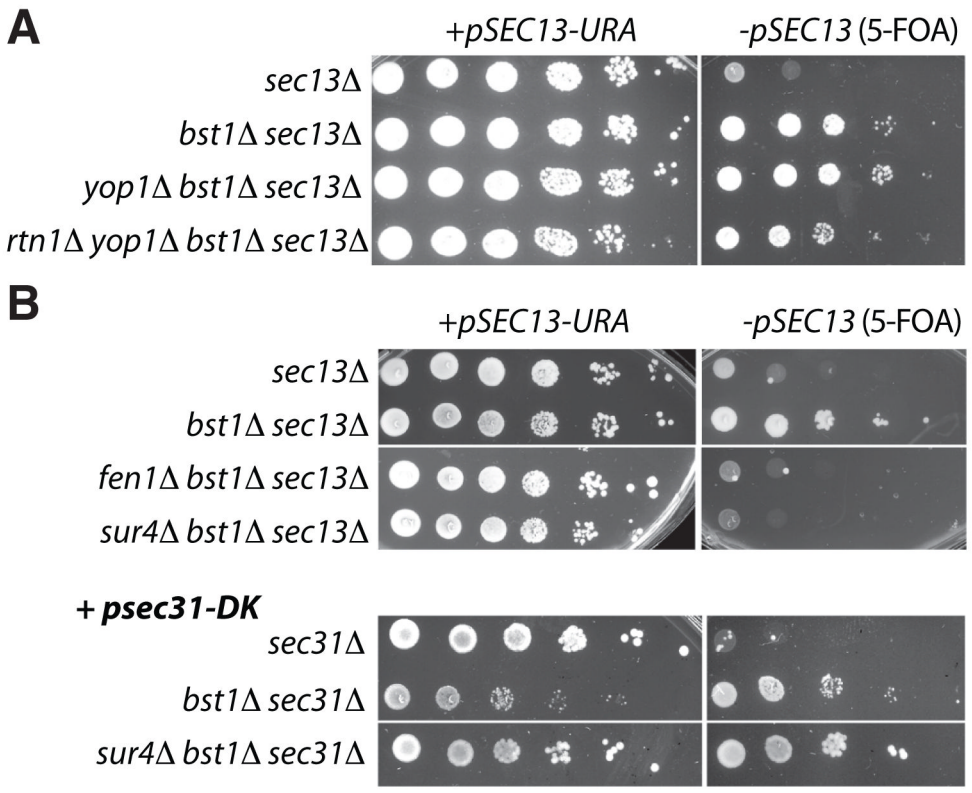

Fig. 3. Global ER curvature is unrelated to Sec13p bypass

(A) Reticulons, which maintain curvature of the ER, are not required for the *bst* phenotype because *bst1Δ sec13Δ* cells are viable when Yop1p and Rtn1p are deleted. **(C)** Likewise, long-chain fatty acid synthases Sur4p and Fen1p are not required for generation of curvature during COPII vesicle formation.

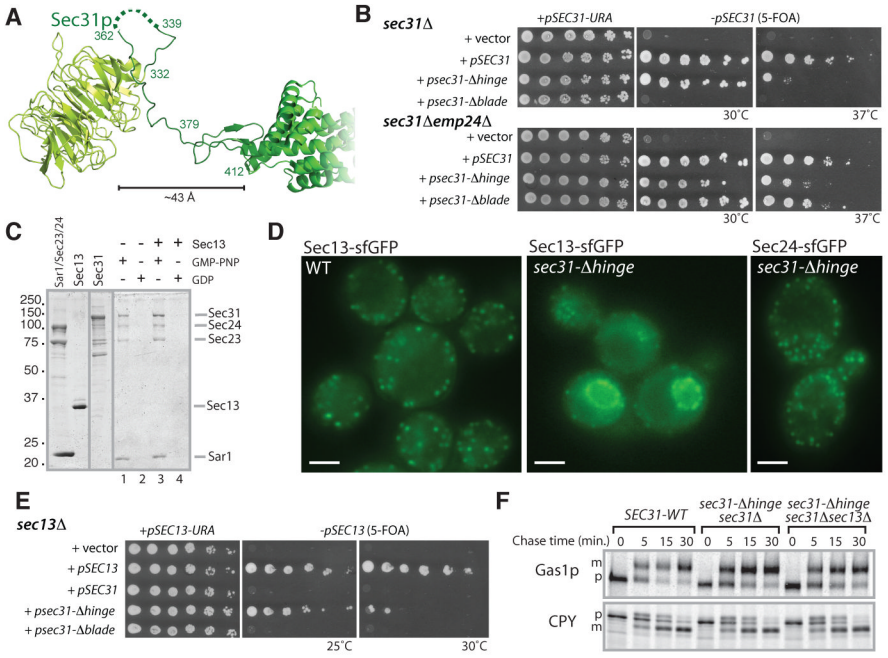

Figure 4. A Sec31p mutant with altered flexibility suggests that Sec13p provides rigidity to the Sec13/31p complex

(A) Structural representation of Sec31p showing the flexible span between the β-propeller and ACE domains, including a region (dotted line) not visualized in the crystal structure. **(B)** Plasmids encoding Sec31p mutants – *psec31-Δblade* (Δ379–412) or *psec31-Δhinge* (Δ332–412) – were introduced into *sec31Δ* and *sec31Δ emp24Δ* strains as indicated and grown on 5-FOA at 30°C and 37°C. **(C)** Sec31p-Δhinge was recruited to COPII-containing liposomes as described in Fig. 1D. **(D)** Sec13p-sfGFP (left and middle panels) redistributed from ER exit sites in wild-type cells (left panel) to the nuclear envelope and cytoplasm in a *sec31-Δhinge* mutant (middle panel); Sec24p-sfGFP localized normally in a *sec13*Δ strain expressing Sec31p-Δhinge (right panel). Scale bar is 2 μm. **(E)** The *sec31-Δhinge* mutant complements a *sec13Δ* strain, permitting growth on 5-FOA at 25°C. **(F)** Maturation of Gas1p and CPY maturation was assessed as described in Fig. 2D.